Internal Medicine
The Japanese Society of Internal Medicine
doi: 10.2169/internalmedicine.7118-21
Intern Med 60: 3129-3136, 2021
http://internmed.jp

【 CASE REPORT 】

Glucocorticoid-dependent Tubulointerstitial Nephritis with IgM-positive Plasma Cells Presenting with Intracellular Crystalline Inclusions within the Rough Endoplasmic Reticulum

Masanori Minato[1], Taichi Murakami[1,2], Naoki Takahashi[3], Hiroyuki Ono[1], Kenji Nishimura[1], Masanori Tamaki[1], Kojiro Nagai[1], Hideharu Abe[1], Masayuki Iwano[3], Kensuke Joh[4] and Toshio Doi[1]

Abstract:

Tubulointerstitial nephritis (TIN) with IgM-positive plasma cells (IgMPC-TIN) is an autoimmune kidney disease characterized by IgM/CD138-double-positive plasma cell infiltration in the tubulointerstitium. A 50-year-old man developed IgMPC-TIN and presented with crystalline inclusions in the rough endoplasmic reticulum. Intracellular crystal formation is a rare finding in paraprotein-related kidney diseases, but this case showed no pathogenic monoclonal immunoglobulin. Prednisolone (PSL, 30 mg) improved the TIN, but PSL tapering resulted in the recurrence of TIN. Combination therapy with 15 mg PSL and 150 mg mizoribine ultimately stabilized TIN. This case offers original evidence concerning the pathophysiology and treatment strategy of IgMPC-TIN.

Key words: tubulointerstitial nephritis with IgM-positive plasma cells, intracellular crystalline inclusions in the rough endoplasmic reticulum, glucocorticoid dependence

(Intern Med 60: 3129-3136, 2021)
(DOI: 10.2169/internalmedicine.7118-21)

Introduction

Recently, tubulointerstitial nephritis (TIN) with IgM-positive plasma cells (IgMPC-TIN) has been proposed as a novel histological entity, and its clinical manifestations have been reported (1). IgMPC-TIN is presumed to be an autoimmune kidney disease that is characterized by several clinical and pathological features, such as a frequent occurrence in women, positivity for anti-mitochondrial antibodies, high serum IgM levels, IgM-positive plasma cell infiltration in the interstitium, and a good response to intermediate-dose glucocorticoids. IgMPC-TIN often occurs in patients with primary biliary cirrhosis/cholangitis (PBC), a chronic cholestatic liver disease. PBC is serologically characterized by positive anti-mitochondrial antibodies and high serum IgM levels. Immunohistochemical examinations have revealed IgM-positive plasma cell infiltration in the portal tract (2). Thus, we hypothesized that IgMPC-TIN might occur as a distinct kidney disease, independent of PBC, and that IgMPC-TIN and PBC might have a common pathological condition.

Since paraproteinemia can produce a spectrum of renal lesions, the pathophysiology of paraprotein-related kidney diseases has been clarified. A rare phenotype is intracellular immunoglobulin crystal formation (3, 4), which is associated with proximal tubular cells (5), interstitial histiocytes (6, 7), and podocytes (8, 9). The crystals are mostly made up of monoclonal κ light chains that are filtered through glomeruli and reabsorbed into each cell. In most cases, monoclonal κ

[1]Department of Nephrology, Tokushima University Graduate School of Biomedical Science, Japan, [2]Department of Nephrology, Ehime Prefectural Central Hospital, Japan, [3]Department of Nephrology, Faculty of Medical Science, University of Fukui, Japan and [4]Department of Pathology, The Jikei University School of Medicine, Japan
Received: January 19, 2021; Accepted: February 16, 2021; Advance Publication by J-STAGE: April 12, 2021
Correspondence to Dr. Taichi Murakami, c-tamurakami@eph.pref.ehime.jp

Table 1. Laboratory Test.

(Peripheral blood)		(Chemical analysis)		(Blood gas analysis)	
White blood cell	4,600 /μL	Amylase	70 U/L	pH	7.361
Neutrophil	71.5 %	Total cholesterol	170 mg/dL	pCO_2	31.1 mmHg
Lymphocyte	17.5 %	HDL cholesterol	40 mg/dL	pO_2	104.6 mmHg
Monocyte	6.5 %	Triglyceride	130 mg/dL	HCO_3^-	17.2 mEq/L
Eosinophil	3.5 %	Blood sugar	110 mg/dL	Anion gap	11.8 mEq/L
Red blood cell	341×10^4 /μL	HbA1c (NGSP)	5.2 %		
Hemoglobin	16.4 g/dL			(Urinalysis)	
Platelet	19.5×10^4 /μL	(Serology)		pH	7.5
		C reactive protein	0.06 mg/dL	Protein	2+
(Chemical analysis)		IgG	1,219 mg/dL	Occult blood	-
AST	13 U/L	IgG4	55.9 mg/dL	Sugar	2+
ALT	14 U/L	IgA	248 mg/dL	Red blood cell	0-1 /HPF
Lactate dehydrogenase	131 U/L	IgM	592 mg/dL	White blood cell	0-1 /HPF
γGTP	36 U/L	IgE	5.6 IU/mL		
Alkaline phosphatase	285 U/L	C3	74 mg/dL	(Urine chemistry)	
Total bilirubin	1.1 mg/dL	C4	21 mg/dL	Protein	0.31 g/day
Total protein	7.6 g/dL	CH50	54 U/mL	Albumin	0.06 g/day
Albumin	4.4 g/dL	Rheumatoid factor	10 U/mL	Glucose	2.14 g/day
Uric acid	2.9 mg/dL	Anti nuclear antibody	×160	NAG	11.6 U/L
Blood urea nitrogen	20 mg/dL	Anti mitochondrial Ab	×80	β2microglobulin	56,316 μg/L
Creatinine	1.51 mg/dL	Anti SS-A Ab	(-)	L-FABP	67.9 μg/gCr
Sodium	138 mEq/L	Anti SS-B Ab	(-)	Urine anion gap	>0 mEq/L
Potassium	4.1 mEq/L	Serum monoclonal	(-)	FEK	11.3 %
Chloride	109 mEq/L	Protein (immunofixation)		FECa	3.2 %
Calcium	9.1 mg/dL	HBs Ag	(-)	TmP/GFR	2.55 mg/dL
Phosphorus	2.7 mg/dL	HCV Ab	(-)	CUA/CCr	20.1 %
Magnesium	2.2 mg/dL				

AST: aspartate transaminase, ALT: alanine aminotransferase, γGTP: γ-glutamyltransferase, HBs Ag: hepatitis B surface antigen, HCV Ab: hepatitis C virus antibody, NAG: N-acetylglucosamine, L-FABP: liver-type fatty acid binding protein, FEK: fractional excretion of potassium, FECa: fractional excretion of calcium, TmP/GFR: tubular phosphorus maximum resorption rate-to-glomerular filtration rate ratio, CUA/CCr: uric acid clearance-to-creatinine clearance ratio

light chains belong to the Vκ1 variability subgroup, and most of them are encoded by the LC02/12 germ-line (10). These κ light chains frequently display an unusual hydrophobic residue at position 30 of the V domain (11). The peculiarities of the variable κ domain can account for the resistance to lysosomal proteolysis and promote self-aggregation and crystallization in lysosomes (12).

We herein report a man with glucocorticoid-dependent IgMPC-TIN who presented with uncommon findings of intracellular crystalline inclusions in the rough endoplasmic reticulum (rER).

Case Report

A 50-year-old man was referred to our hospital for the evaluation of an elevated serum creatinine level of 1.44 mg/dL. This patient had a history of proteinuria and glycosuria for 10 years before the first visit. However, he had no contributory medical history, including neither hypertension nor diabetes mellitus, and was on no medication. He had a history of smoking (10 cigarettes/day for 30 years).

No abnormal physical findings were observed on a physical examination. Laboratory data are shown in Table 1. The patient's urinalysis revealed a urine pH of 7.5, no hematuria, mild proteinuria of 0.31 g/day, glycosuria of 2.14 g/day, increased excretion of uric acid, elevated β_2 microglobulin of 56,316 μg/L, and elevated L-type fatty acid-binding protein of 67.9 μg/gCr. A blood gas analysis revealed a pH of 7.361, a pCO_2 of 31.1 mmHg, and an HCO_3- concentration of 17.2 mEq/L, suggesting mild metabolic acidosis. These data imply tubular injury accompanied by renal tubular acidosis. Blood tests further revealed hypouricemia with 2.9 mg/dL, an elevated IgM level of 592 mg/dL, positivity for anti-nuclear antibodies, and elevated anti-mitochondrial antibodies at ×160. These data indicated autoimmune tubulointerstitial nephritis. However, Sjögren syndrome, sarcoidosis, and IgG4-related kidney disease manifested by kidney involvement of tubulointerstitial nephritis were serologically excluded. Serum liver and biliary enzyme levels were within the normal range, and abdominal ultrasonography showed no hepatic abnormality, although anti-mitochondrial antibodies were specific to PBC.

A kidney biopsy was performed for a definitive diagnosis. Light microscopy revealed 13 glomeruli, 8 of which were globally sclerotic. The non-sclerotic glomeruli showed minor glomerular abnormality. Diffuse and moderate fibrosis, focal

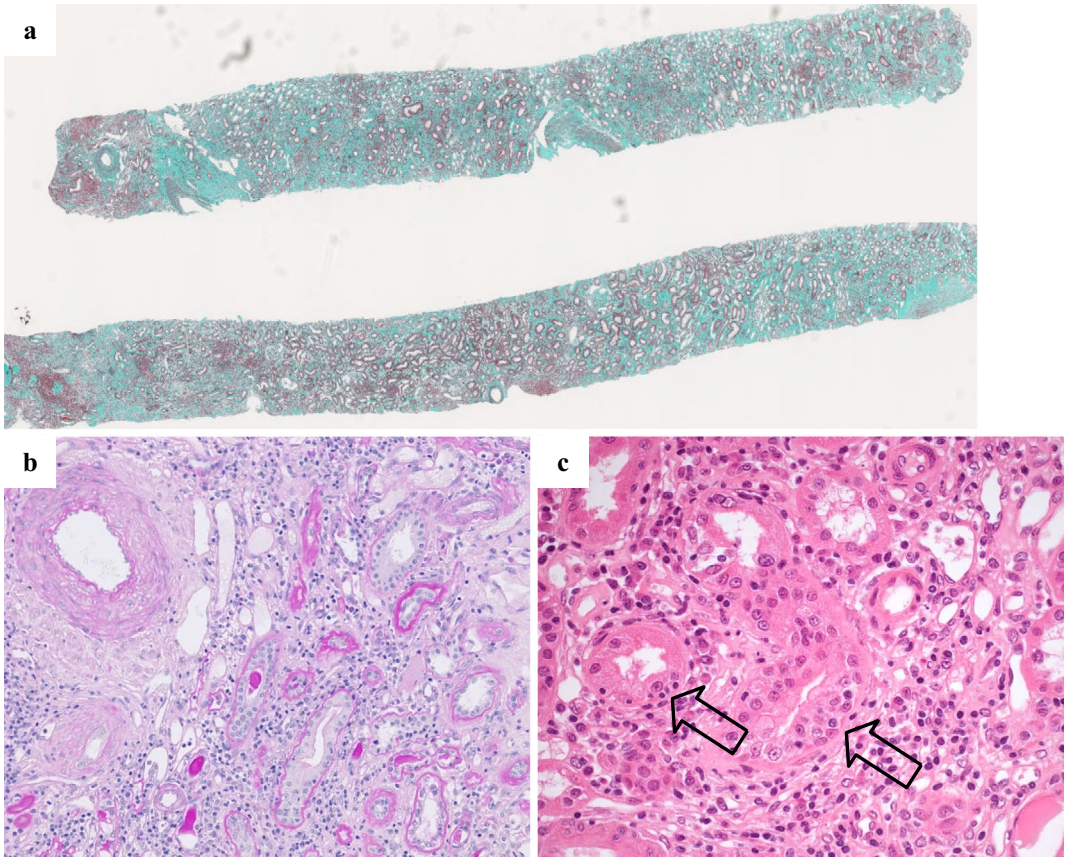

Figure 1. Light microscopic findings. Light microscopy showed the characteristic features of interstitial nephritis and tubulitis. Diffuse and moderate tubulointerstitial fibrosis (a, Masson Trichrome staining) and focal lymphocyte infiltration and tubular atrophy in the interstitium (b, Periodic acid-Schiff staining, ×200) were observed. Mononuclear lymphocytes had infiltrated between tubular epithelial cells (arrows in c, Hematoxylin and Eosin staining, ×400).

immunocyte infiltration and tubular atrophy in the tubulointerstitium were observed (Fig. 1a, b). Mononuclear lymphocytes infiltrated into tubules, thus suggesting tubulitis (Fig. 1c). No immune deposits were detected in the glomeruli or in the interstitium by routine immunofluorescence of fresh-frozen sections. Immunohistochemistry of formalin-fixed, paraffin-embedded specimens revealed inflammatory cell infiltration in the tubulointerstitium, where CD3-positive T cells were predominantly observed. CD138-positive plasma cells in the interstitium were mostly negative for IgG (Fig. 2). Dual immunostaining with IgM and CD138 using formalin-fixed, paraffin-embedded specimens after antigen retrieval was performed in the current case and in a control case (drug-induced TIN) (Fig. 3). IgM/CD138-dual positive plasma cell infiltration was clearly increased in this case compared with a control TIN case. Based on these findings, this patient was diagnosed with IgMPC-TIN.

Electron microscopy revealed club-shaped crystalline structures in the interstitium. At a higher magnification, the crystalline structures were shown to be surrounded by a dilated unit membrane that bounds to ribosomes, thus suggesting intracellular crystalline inclusions within the rER. The crystalline inclusions exhibited striated structures 6-7 nm in width with a center-to-center distance of 10-13 nm (Fig. 4). An abnormal mitochondrial morphology was not observed in the tubular epithelial cells.

The clinical course is shown in Fig. 5. Immunosuppressive therapy with 30 mg of prednisolone (PSL) was initiated. Urine protein, urine sugar, urine β_2 microglobulin, serum IgM, and the estimated glomerular filtration rate (eGFR) were assessed as therapeutic markers. After PSL administration, the eGFR increased, concurrently with the improvement of IgM, urine β_2 microglobulin, and urine sugar level. However, PSL tapering led to a decrease in the eGFR with worsening of findings for serum and urine markers. Thus, the intensification of therapy with a combined administration of 20 mg PSL and 75 mg cyclosporine A or 150 mg mizoribine was tested. This combination therapy was more effective than PSL monotherapy, although the decrease in PSL resulted in the deterioration of urine markers. Ultimately, 15 mg PSL with 150 mg mizoribine resulted in the stabilization of TIN, with normalized urine sugar and protein levels and low urine β_2 microglobulin levels; the eGFR did not markedly deteriorate during the follow-up period.

Discussion

The characteristic pathological findings of IgMPC-TIN

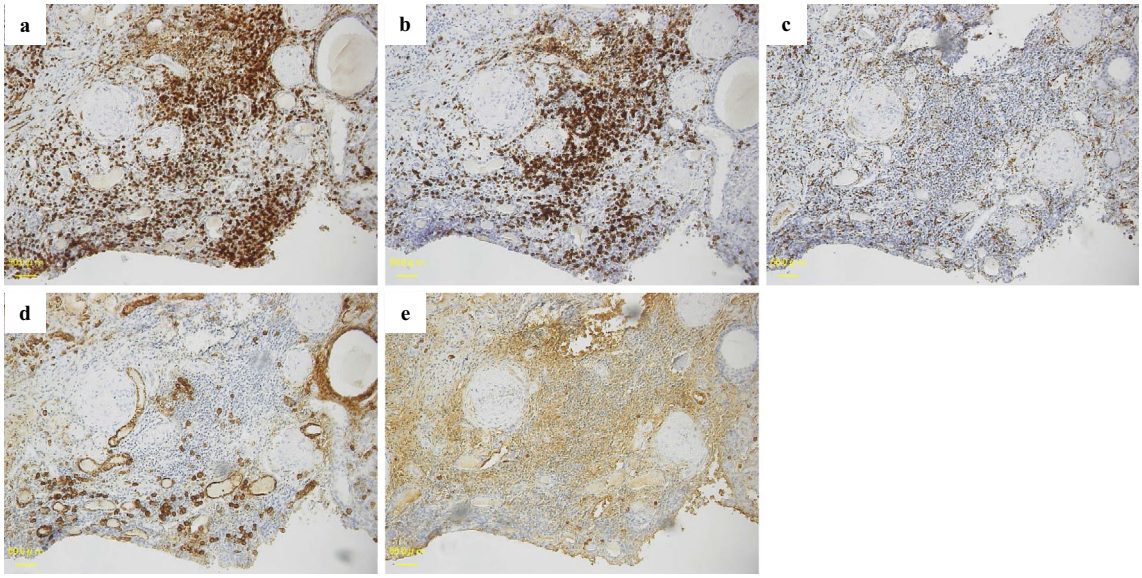

Figure 2. **Immunohistochemistry. Immunohistochemistry shows dominant CD3-positive T cell infiltration in the tubulointerstitium (a-d). CD138-positive plasma cells in the interstitium were largely negative for IgG (d, e). a-e show the same area in the cortex. Immunostaining was performed for formalin-fixed, paraffin-embedded specimens after antigen retrieval (a: CD3, b: CD20, c: CD68/PGM-1, d: CD138, e: IgG).**

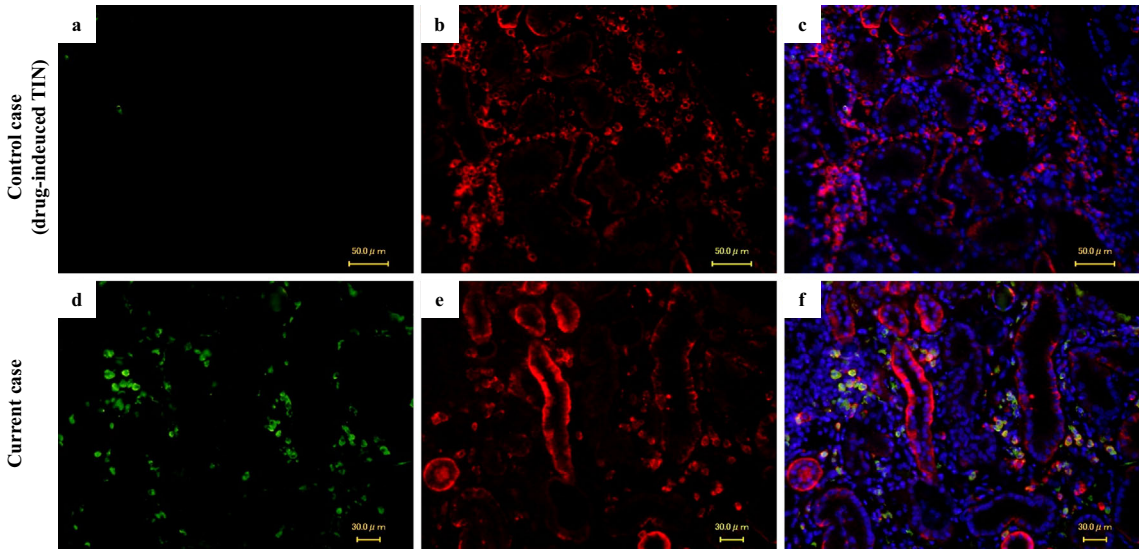

Figure 3. **Dual immunostaining with IgM and CD138. Immunofluorescent staining revealed the infiltration of CD138-positive plasma cells labeled with IgM in the interstitium in the current case. The control case with drug-induced TIN showed the predominant infiltration of IgM-negative plasma cells. a/d: IgM, b/e: CD138, c/f: IgM/CD138/DAPI. DAPI: 4',6-diamidino-2-phenylindole**

are diffuse interstitial distribution of CD3-positive T lymphocytes and infiltrating IgM-positive plasma cells in the interstitium, as proven using dual immunostaining with CD 138 and IgM (1). In particular, IgM-positive plasma cell infiltration is critical for a definitive diagnosis, as infiltration of IgG-positive plasma cells is a common finding in TIN (13). Therefore, in the present case, we revealed the co-expression of IgM (55199; CAPPEL, Ohio, USA) and CD 138 (M7228; DAKO, Hovedstaden, Denmark) on formalin-fixed, paraffin-embedded specimens after antigen retrieval (06380-05; Nacalai Tesque, Kyoto, Japan) using immunofluorescence. We confirmed that plasma cells were largely negative for IgM in control TIN specimens using the same method. In addition, we also observed similar results using immunohistochemistry with different anti-human IgM antibody (IR513; DAKO) (Supplementary material). We assumed that the epitopes of IgM expressed by immune deposits and plasma cells were different, so the detection of IgM expressed by plasma cells might require antigen retrieval process to clearly detect.

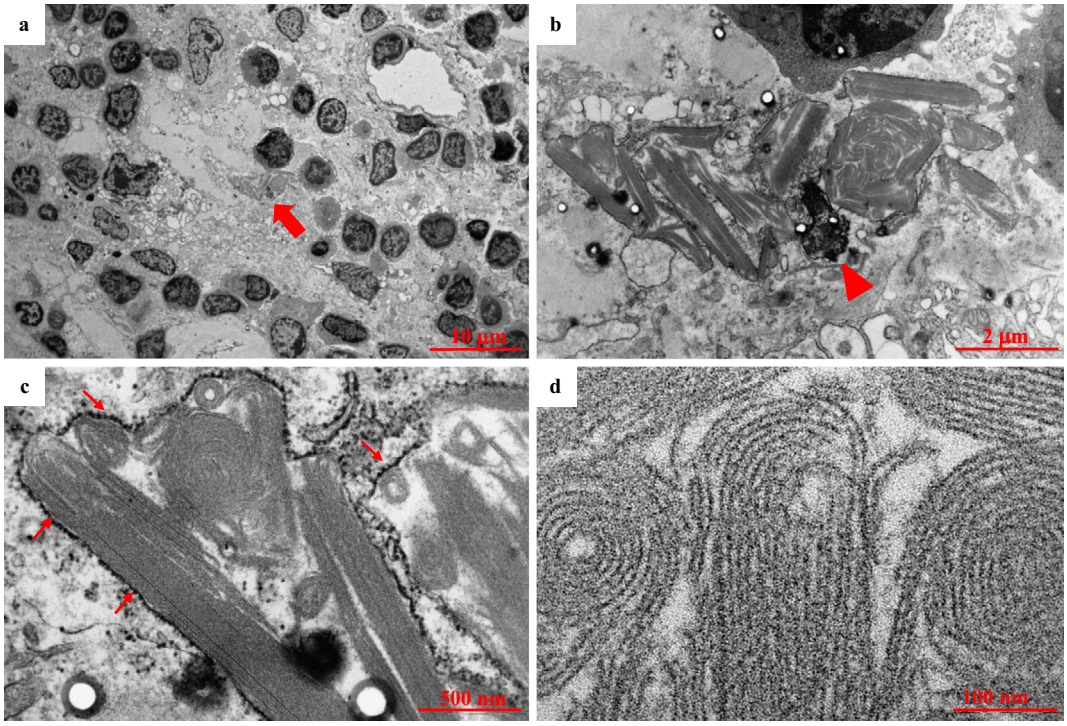

Figure 4. **Electron microscopic findings. Intracellular club-shaped crystalline inclusions were observed in interstitial cells (a, arrow). The arrowhead indicates the nucleus in b. The arrows show the membrane-bound ribosomes, suggesting that crystals were included in the distended rough endoplasmic reticulum (c). At a higher magnification, crystalline inclusions exhibited striated structures 6-7 nm in width with a center-to-center distance of 10-13 nm (d).**

Intriguingly, the current case showed crystalline inclusions in the rER in interstitial cells. Immunoglobulins can accumulate intracellularly to form protein crystals under certain physiological conditions or disease settings. There are two types of intracellular immunoglobulin crystallization. One type occurs in the endosome/lysosome compartments, where phagocytosed or reabsorbed immunoglobulins traffic for recycling into circulation or for degradation. Crystallin inclusions are formed during the catabolic process of immunoglobulins due to their resistance to lysosomal proteolysis. The other type of crystallization occurs in the rER, where immunoglobulin synthesis, folding, and assembly occur (14). To our knowledge, crystalline inclusion in the rER associated with kidney diseases has never been reported. However, 17 previous reports described crystalline inclusions in the rER in a variety of disease settings (Table 2) (15-31). Most of these were neoplastic and inflammatory diseases. Eight reports were associated with plasma cell dyscrasia. Six of 11 reports associated with lymphocytic cells described the detection of immunoglobulin-derived crystals. No particular subclasses of the heavy chain were detected in these reports; however, the light chain subclass was λ chain in four reports and κ chain in one report. These data suggest that lymphocytic cells actively producing immunoglobulins can form intra-rER crystals composed of heavy and light chains with peculiar physicochemical conditions.

The details of immunoglobulin crystal formation in the rER remain to be fully elucidated. Goldberg originally speculated that intracellular crystals were composed of structurally abnormal immunoglobulins that cells were unable to secrete (32). However, a recent *in vitro* study proposed that crystallization was the direct consequence of biosynthetic activities in immunoglobulin-producing cells (33). CHO cells stably transfected with a full-length normal human IgG clone spontaneously induced the formation of rod-shaped crystals in the rER lumen. The intra-ER crystals were composed of reversibly soluble and correctly assembled and folded IgG. Likewise, intracellular crystal-derived IgG retained an antigen binding ability equivalent to that of secreted IgG. In addition, transiently transfected HEK293 cells developed intracellular crystals when ER export was blocked by brefeldin A. The authors concluded that export-ready IgG accumulated progressively in the ER lumen until a threshold concentration, necessary to nucleate the crystals, was reached. IgMPC-TIN is not plasma cell dyscrasia, but interstitial plasma cells were found to overproduce IgM in the current case. In addition, crystalline inclusions in our case showed striated structures that were 6-7 nm in width with a center-to-center distance of 10-13 nm. Some previous reports have described unusual extracellular deposits of crystals that exhibited striated structures (34, 35). Crystals in rER also have been reported to exhibit filament or tubular structures with regular periodicity (19, 20, 22, 26, 28, 30). Plasmacytic lymphocytes synthesized IgG-derived crystals in rER that exhibited striated structures with a periodicity of 8 nm, which was similar to that in the current case. We specu-

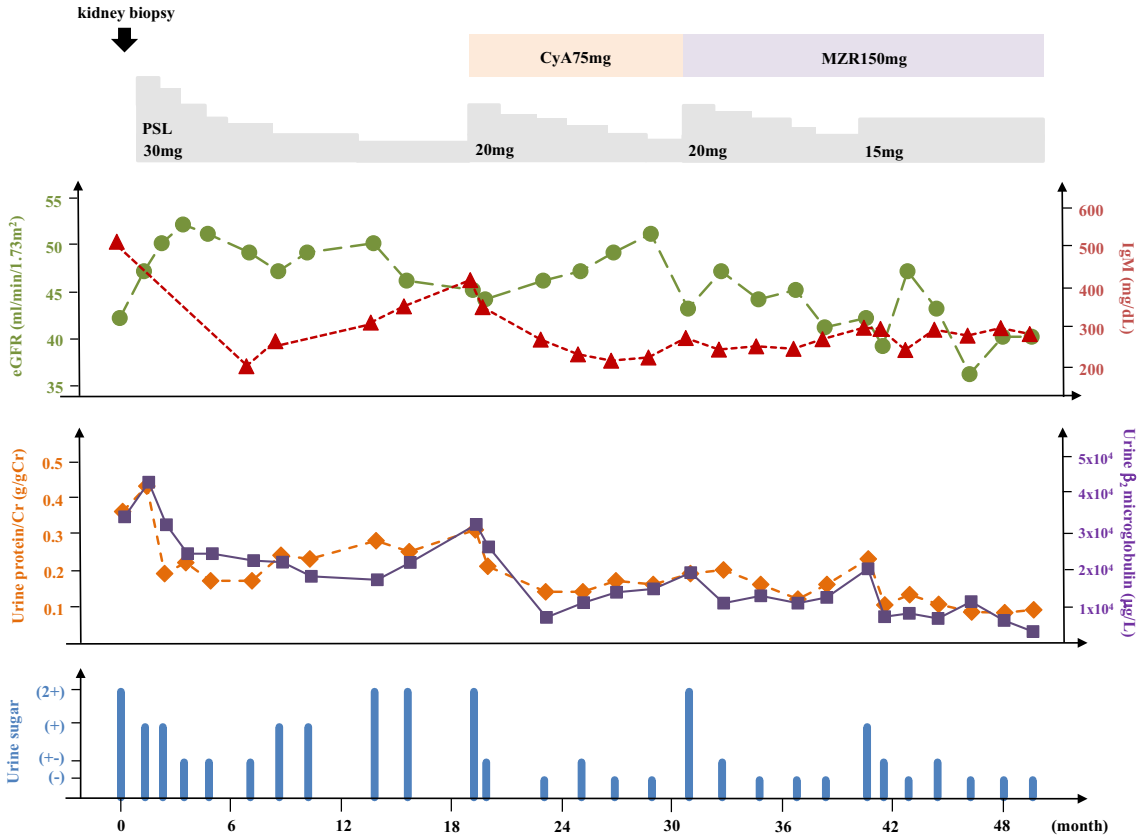

Figure 5. **Clinical course. PSL (30 mg) alone increased the eGFR, accompanied by the improvement of IgM, β2 microglobulin, and urinary sugar levels; however, PSL tapering resulted in a decrease in the eGFR with worsening of serum and urine markers. Thus, the combined administration of 20 mg PSL and 75 mg cyclosporine A or 150 mg mizoribine was tested. The combination therapy was more effective than PSL monotherapy, although the decrease in PSL resulted in the deterioration of urine markers. Finally, 15 mg PSL with 150 mg mizoribine normalized urine sugar and protein levels and improved urine β2 microglobulin levels despite slightly decreasing the eGFR in the follow-up period. PSL: prednisolone, CyA: cyclosporine A, MZR: mizoribine, eGFR: estimated glomerular filtration rate, Cr: creatinine**

lated that the intra-ER crystals developed in interstitial plasma cells that actively synthesized IgM. This is a rare cellular phenomenon in inflammatory kidney diseases.

The optimal regimen of immunosuppressive therapy for IgMPC-TIN has not been determined, and the long-term renal prognosis is still unknown. However, we reported that patients with IgMPC-TIN receiving an intermediate dose of glucocorticoids often respond to the therapy, and their renal function was preserved at the last follow-up (0.2-15.0 years) (1). The current patient responded to 30 mg of glucocorticoids, with repeated recurrence after PSL tapering to less than 10 mg. We considered that urinary sugar, protein, and β2 microglobulin as well as serum IgM levels were useful biomarkers of disease activity. After the first recurrence, the combined administration of 20 mg of PSL with cyclosporine A or mizoribine was initiated. Combination therapy with glucocorticoids and immunosuppressants improved disease biomarkers more effectively than glucocorticoid monotherapy. In the follow-up period, 15 mg of PSL with 150 mg of mizoribine tentatively stabilized the disease activity. However, further tapering of glucocorticoids should be considered, and long-term follow-up is required to validate the effect of combined therapy in IgMPC-TIN. A few cases of recurrent IgMPC-TIN have been reported. Matsuoka-Uchiyama et al. reported two cases of relapse after rapid tapering of glucocorticoids (36). Mizoguchi et al. reported a case of recurrent IgMPC-TIN associated with PBC after steroid tapering that improved following the administration of 500 mg of methylprednisolone per day for 3 consecutive days, followed by 10 mg of PSL daily (37). Further evidence will be required to determine the ideal regimen for improving the long-term prognosis in glucocorticoid-dependent IgMPC-TIN.

In conclusion, we encountered a man with recurrent IgMPC-TIN presenting with crystalline inclusions in the rER. This case may add further evidence to the pathophysiology and treatment strategy of IgMPC-TIN.

Informed consent was obtained from all of the individual participants included in the study.

All procedures performed in the studies involving human par-

Table 2. Previous Reports Describing Crystalline Inclusions in Rough Endoplasmic Reticulum.

Year/Ref.	Diagnosis	Organ	Cell type or tissue	Origin of crystal
1971/15	Hodgkin's disease	Lymph node	Lymphoma cell	Undetermined
1973/16	Chronic lymphocytic leukemia	Peripheral blood	Leukemia cell	IgMλ
1973/17	Chronic lymphocytic leukemia	Peripheral blood	Leukemia cell	IgAλ
1975/18	Multiple myeloma Macroglobulinemia	Bone marrow	Myeloma cell	Undetermined
1976/19	Multiple sclerosis	Brain	Astrocyte	undetermined
1980/20	Papillary conjunctivitis	Eye	Plasmacytic Lymphocyte	IgG
1982/21	Chronic lymphocytic leukemia	Peripheral blood	Leukemia cell	IgMλ
1982/22	Lymphoproliferative disorder	Peripheral blood	Lymphocyte	Undetermined
1984/23	Malakoplakia	Stomach, submental region, Oropharyngeal soft tissue	Plasmacytoid cell	Undetermined
1986/24	Non-hodgkin lymphoma	Stomach	Lymphoma cell	Undetermined
1987/25	Plasmacytoma	Stomach	Plasmacytoma cell	IgMλ
1987/26	Atrial myxoma	Heart	Myxoma cell	Undetermined
1990/27	Osteosarcoma	Bone	Osteosarcoma cell	Undetermined
1992/28	HIV infection	Placenta	Syncytiotrophoblast	Human placental lactogen
1995/29	Giant-cell fibroblastoma	Nose	Fibroblastoma cell	Vimentin
2002/30	Adrenal cortical tumor	Adrenal gland	Adrenal tumor cell	Undetermined
2007/31	Multiple myeloma	Bone marrow	Myeloma cell	IgGκ
present case	IgMPC-TIN	Kidney	Undetermined	Undetermined

HIV: human immunodeficiency virus, IgMPC-TIN: tubulointerstitial nephritis with IgMpositive plasma cells

ticipants were in accordance with the ethical standards of the institutional and/or national research committee at which the studies were conducted (IRB approval number 680-1) and with the 1964 Declaration of Helsinki and its later amendments or comparable ethical standards.

The authors state that they have no Conflict of Interest (COI).

References

1. Takahashi N, Saeki T, Komatsuda A, et al. Tubulointerstitial nephritis with IgM-positive plasma cells. J Am Soc Nephrol **28**: 3688-3698, 2017.
2. Daniels JA, Torbenson M, Anders RA, Boitnott JK. Immunostaining of plasma cells in primary biliary cirrhosis. Am J Clin Pathol **131**: 243-249, 2009.
3. Doshi M, Lahoti A, Danesh FR, Batuman V, Sanders PW. Paraprotein-related kidney disease: kidney injury from paraproteins - what determines the site of injury? Clin J Am Soc Nephrol **11**: 2288-2294, 2016.
4. Bridoux F, Leung N, Hutchison CA, et al. Diagnosis of monoclonal gammopathy of renal significance. Kidney Int **87**: 698-711, 2015.
5. Stokes MB, Valeri AM, Herlitz L, et al. Light chain proximal tubulopathy: clinical and pathologic characteristics in the modern treatment era. J Am Soc Nephrol **27**: 1555-1565, 2016.
6. Stokes MB, Aronoff B, Siegel D, D'Agati VD. Dysproteinemia-related nephropathy associated with crystal-storing histiocytosis. Kidney Int **70**: 597-602, 2006.
7. El Hamel C, Thierry A, Trouillas P, et al. Crystal-storing histiocytosis with renal Fanconi syndrome: pathological and molecular characteristics compared with classical myeloma-associated Fanconi syndrome. Nephrol Dial Transplant **25**: 2982-2990, 2010.
8. Matsuyama N, Joh K, Yamaguchi Y, et al. Crystalline inclusions in the glomerular podocytes in a patient with benign monoclonal gammopathy and focal segmental glomerulosclerosis. Am J Kid Dis **23**: 859-865, 1994.
9. Nasr SH, Preddie DC, Markowitz GS, Appel GB, D'Agati VD. Multiple myeloma, nephrotic syndrome and crystalloid inclusions in podocytes. Kidney Int **69**: 616-620, 2006.
10. Messiaen T, Deret S, Mougenot B, et al. Adult Fanconi syndrome secondary to light chain gammopathy. Clinicopathologic heterogeneity and unusual features in 11 patients. Medicine (Baltimore) **79**: 135-154, 2000.
11. Aucouturier P, Bauwens M, Khamlichi AA, et al. Monoclonal Ig L chain and L chain V domain fragment crystallization in myeloma-associated Fanconi's syndrome. J Immunol **150**: 3561-3568, 1993.
12. Leboulleux M, Lelongt B, Mougenot B, et al. Protease resistance and binding of Ig light chains in myeloma-associated tubulopathies. Kidney Int **48**: 72-79, 1995.
13. Saeki T, Kawano M. IgG4-related kidney disease. Kidney Int **85**: 251-257, 2014.
14. Hasegawa H. Aggregates, crystals, gels, and amyloids: intracellular and extracellular phenotypes at the crossroads of immunoglobulin physicochemical property and cell physiology. Int J Cell Biol **2013**: 604867, 2013.
15. Uzman BG, Saito H, Kasac M. Tubular arrays in the endoplasmic reticulum in human tumor cells. Lab Invest **24**: 492-498, 1971.
16. Clark C, Rydell RE, Kaplan ME. Frequent association of IgMlambda with crystalline inclusions in chronic lymphatic leukemic lymphocytes. N Engl J Med **289**: 113-117, 1973.
17. Cawley JC, Barker CR, Britchford RD, Smith JL. Intracellular IgA immunoglobulin crystals in chronic lymphocytic leukaemia. Clin Exp Immunol **13**: 407-416, 1973.
18. Oikawa K. Electron microscopic observation of inclusion bodies in plasma cells of multiple myeloma and Waldenström's macroglobulinemia. Tohoku J Exp Med **117**: 257-281, 1975.
19. Johnson T, Knobeloch L, Sunderland E, et al. Crystals, paracrystals, and rigid tubules in multiple sclerotic brain and spinal fluid. Lab Invest **35**: 264-271, 1976.

20. Rao NA, Font RL. Plasmacytic conjunctivitis with crystalline inclusions. Immunohistochemical and ultrastructural studies. Arch Ophthalmol **98**: 836-841, 1980.
21. Ralfkiaer E, Hou-Jensen K, Geisler C, Plesner T, Henschel A, Hansen MM. Cytoplasmic inclusions in lymphocytes of chronic lymphocytic leukaemia. A report of 10 cases. Virchows Arch A Pathol Anat Histol **395**: 227-236, 1982.
22. Sun CN, Amir J, White HJ. Crystalline inclusions within rough endoplasmic reticulum and perinuclear space of human lymphocytes. Cytologia (Tokyo) **47**: 219-225, 1982.
23. Flint A, Murad TM. Malakoplakia and malakoplakialike lesions of the upper gastrointestinal tract. Ultrastruct Pathol **7**: 167-176, 1984.
24. Irro F, Gütz HJ, Marx G. [Signet-ring-cell lymphoma. Light and electron microscopic study of gastric involvement]. Arch Geschwulstforsch **56**: 263-268, 1986 (in German, Abstract in English).
25. Kobayashi Y, Miyake T, Funakoshi N, Kanoh T, Uchino H. Gastric plasmacytoma with cylindrical crystalline inclusions. Gastroenterol Jpn **22**: 81-87, 1987.
26. Powell HC, Weissinger J. Intracysternal crystalline cytoplasmic inclusions in a cardiac myxoma. Am J Cardiovasc Pathol **1**: 135-140, 1987.
27. Murray AB, Becke H, Taccagni GL. Extraskeletal osteosarcoma with unusual ultrastructural features. Ultrastruct Pathol **14**: 335-342, 1990.
28. Drachenberg CB, Papadimitriou JC. Endocrine secretory granules and crystals in the syncytiotrophoblast. J Submicrosc Cytol Pathol **24**: 123-127, 1992.
29. Bosman C, Boldrini R, Pierro V, Corsi A. Unusual ultrastructural findings in giant-cell fibroblastoma. Tumori **81**: 283-289, 1995.
30. Seo IS, Henley JD, Min KW. Peculiar cytoplasmic inclusions in oncocytic adrenal cortical tumors: an electron microscopic observation. Ultrastruct Pathol **26**: 229-235, 2002.
31. Kobayashi C, Tanabe J, Aoki M, et al. [IgG-kappa type multiple myeloma with cytoplasmic crystalline inclusions]. Rinsho Ketsueki **48**: 652-658, 2007 (in Japanese).
32. Goldberg AF. An unusual lymphomatous disease associated with intracytoplasmic crystals in lymphoplasmocytoid cells. Blood **16**: 1693-1707, 1960.
33. Hasegawa H, Wendling J, He F, et al. *In vivo* crystallization of human IgG in the endoplasmic reticulum of engineered Chinese hamster ovary (CHO) cells. J Biol Chem **286**: 19917-19931, 2011.
34. Ohtani H, Wakui H, Komatsuda A, et al. Progressive glomerulopathy with unusual deposits of striated structures: a new disease entity? Nephrol Dial Transplant **25**: 2016-2019, 2010.
35. Yamamoto T, Togawa A, Eguchi M, et al. Glomerulopathy with distinctive fibrillar deposits but lacking glomerular deposition of type III collagen. CEN Case Rep **5**: 163-167, 2016.
36. Matsuoka-Uchiyama N, Tsuji K, Fukushima K, et al. Tubulointerstitial nephritis cases with IgM-positive plasma cells. Kidney Int Rep **5**: 1576-1580, 2020.
37. Mizoguchi S, Katayama K, Murata T, et al. IgM-positive tubulointerstitial nephritis associated with asymptomatic primary biliary cirrhosis. Kidney Int Rep **3**: 1004-1009, 2018.